JOURNAL
OF
GEOMAGNETISM
AND
GEOELECTRICITY

VOL. II NO. 1

SOCIETY
OF
TERRESTRIAL MAGNETISM AND ELECTRICITY

May 1950

KYOTO

On the Influence of the Hall Current to the Electrical Conductivity of the Ionosphere. I

By Motokazu HIRONO

Geophysical Institute, Kyoto University

Abstract

Direct electrical conductivity of the ionosphere is examined mainly concerning the effect of Hall current. It is suggested that the effect of the electric field produced by vertical component of the Hall current, together with the smaller effect by its horizontal component, may construct, along the magnetic equator in the ionosphere, a narrow region, in which the conductivity near the level of the E layer is much greater than in the other latitudes. This result is considered to be very fit for the distribution with latitudes of the range of diurnal variation of the terrestrial magnetism.

1. General formulae. It is well known that the presence of a transverse magnetic field causes certain anomalies in the flow of electric currents in ionized gases. When an electromotive force is applied in the gases, the Hall current tends to flow, and that reduces the conductivity of the material. We shall here evaluate the magnitude of the effects in the ionosphere. We represent charged particles and neutral particles, by suffix 1,2 respectively and let $\boldsymbol{c}_1$, $\boldsymbol{c}_2$ be velocities of particles, n_1, n_2 be number densities, m_1, m_2 be masses, then mass velocity $\boldsymbol{c}_0$ can be written as

$$\boldsymbol{c}_0 \equiv (n_1 m_1 \boldsymbol{c}_1 + n_2 m_2 \boldsymbol{c}_2)/(n_1 m_1 + n_2 m_2) \tag{1}$$

As in the E and F layer, the number of neutral particles is much greater than that of charged particles, we may put $\boldsymbol{c}_0 \simeq \boldsymbol{c}_2$.

Boltzmann's equation for the first gas is [1]

$$\frac{Df_1}{Dt} + \boldsymbol{C}_1 \cdot \frac{\partial f_1}{\partial \boldsymbol{r}} + \left(\boldsymbol{F}_1 + \frac{e_1}{m_1} \boldsymbol{c}_0 \times \boldsymbol{H} - \frac{D\boldsymbol{c}_0}{Dt} \right) \cdot \frac{\partial f_1}{\partial \boldsymbol{C}_1} + \frac{e_1}{m_1} (\boldsymbol{C}_1 \times \boldsymbol{H}) \cdot \frac{\partial f_1}{\partial \boldsymbol{C}_1} - \frac{\partial f_1}{\partial \boldsymbol{C}_1} \boldsymbol{C}_1 : \frac{\partial}{\partial \boldsymbol{r}} \boldsymbol{c}_0 = -J_1(ff_1) - J_{12}(f_1 f_2)$$

We get a first approximate solution $f_1^{(1)}$ of this equation under the assumption that the temperature is everywhere uniform and $(\partial/\partial \boldsymbol{r})\boldsymbol{c}_0$ is negligible. Using the relation: $\bar{\boldsymbol{C}}_1 = \frac{1}{n_1} \int f_1^{(1)} \boldsymbol{C}_1 d\boldsymbol{c}_1$ we get the next equation.

$$\begin{cases} \bar{\boldsymbol{C}}_1 = -\dfrac{p\tau_1}{\rho_1} \cdot \dfrac{\boldsymbol{d}_{12}^{\perp} - (\omega\tau_1/H)\boldsymbol{H} \times \boldsymbol{d}_{12}}{1+\omega^2\tau_1^2} - \dfrac{n^2}{n_1 n_2} D_{12} \boldsymbol{d}''_{12} \\ \bar{\boldsymbol{C}}_2 \simeq 0 \end{cases} \tag{2}$$

where p=pressure $\quad \boldsymbol{H}$=the earth's magnetic field

$\boldsymbol{C}$=peculiar velocity, $\boldsymbol{C}_1=\boldsymbol{c}_1-\boldsymbol{c}_0$, $\boldsymbol{C}_2=\boldsymbol{c}_2-\boldsymbol{c}_0$

$\omega=e_1H/m_1 \qquad \tau_1=1/\nu_1=m_1m_2nD_{12}/kT$

n=number density$=n_1+n_2$

D_{12}=diffusion coefficient for ion: we adopted the value by Sutherland's model of inverse fifth law, considering the effect of electric charge [2]. In this calculation the molecular weights of neutral molecules and ions are both taken to be 20.

e_1=electric charge of particle 1 (emu):

for positive ion $e_1=e$, for electron $e_1=-e$

and $$\boldsymbol{d}_{12}=\frac{\partial}{\partial \boldsymbol{r}}\left(\frac{n_1}{n}\right)+\frac{n_1n_2(m_2-m_1)}{n\rho p}\frac{\partial p}{\partial \boldsymbol{r}}-\frac{\rho_1\rho_2(\boldsymbol{F}_1-\boldsymbol{F}_2)}{\rho p}-\frac{n_1n_2}{\rho p}m_2e_1(\boldsymbol{c}_0\times\boldsymbol{H}) \qquad (3)$$

in which $m_1\boldsymbol{F}_1$, $m_2\boldsymbol{F}_2$ are external forces acting on charged and neutral rarticles, and $\boldsymbol{d}_{12}=\boldsymbol{d}^{\perp}_{12}+\boldsymbol{d}''_{12}$, $\boldsymbol{d}^{\perp}_{12}$ and $\boldsymbol{d}''_{12}$ are components of $\boldsymbol{d}_{12}$ perpendicular and parallel to the magnetic field respectively.

In the E and $F1$ region, according to numerical calculation, the first and the second term of (3) is small compared with the other terms, and in the third term, as the effect of the gravity does not appear, we may take only the effect of the electric field,

therefore $$\boldsymbol{d}_{12}=-\frac{n_1\rho_2e_1}{\rho p}(\boldsymbol{E}^{(s)}+\boldsymbol{c}_0\times\boldsymbol{H}) \qquad (4)$$

where $\boldsymbol{E}^{(s)}$ represents electric field. Let $\boldsymbol{E}=\boldsymbol{E}^{(s)}+\boldsymbol{c}_0\times\boldsymbol{H}$

then (3) becomes

$$\bar{\boldsymbol{C}}_1=\frac{e_1}{m_1}\cdot\frac{\tau_1}{1+\omega_1^2\tau_1^2}\left\{\boldsymbol{E}^{\perp}-\frac{\omega_1\tau_1}{H}(\boldsymbol{H}\times\boldsymbol{E})\right\}+\frac{e_1\tau_1}{m_1}\boldsymbol{E}'' \qquad (5)$$

where $\boldsymbol{E}=\boldsymbol{E}^{\perp}+\boldsymbol{E}''$, $\boldsymbol{E}^{\perp}$ and $\boldsymbol{E}''$ are components of $\boldsymbol{E}$ perpendicular and parrallel to the magnetic field respectively.

2. Consideration on the Hall current.

From (5), charged particles have to move not only in the direction of $\boldsymbol{E}^{\perp}$, $\boldsymbol{E}''$ but also in the direction of $\boldsymbol{E}\times\boldsymbol{H}$. If velocities of ions and electrons in the direction of $\boldsymbol{E}\times\boldsymbol{H}$ are equal, electric current does not flow in this direction. But if these velocities are unequal, the "Hall Current" (in place of which we write H.C. in the following.) flows in this direction. As the ionosphere is considered to form strata horizontally, when an electro-motive force, which, for example produces diurnal variation of terrestrial magnetism, acts in the layer, a vertical component of the H.C. is shown to come not to flow after a very short time, on account of the vertical electric field due to polarization by the H.C.

On the other hand, it is not easily shown whether the horizontal component of the H.C. flows freely or does not flow at all, counteracted by resulting electric field and perhapse the case will be intermediate of these. Therefore we examined the next two cases: (a) Only vertical component of H.C. does not flow.

(b) The H.C. does not flow in any direction.

T.G. Cowling [3] in 1933 showed, in the chromosphere of the sun, that if the

H.C. cannot flow, counteracted by resulting electric field, the conductivity takes the same value as if the transverse magnetic field is absent. But in the case of the ionosphere, as we cannot consider an ideal case that charged particles do not flow at all in the direction of $\boldsymbol{E}\times\boldsymbol{H}$, we shall treat the problem more precisely.

3. Equation of conductivity.

Let right-handed rectangular axis o-xys be taken, so placed that ox, oy, oz are directed to the south, east and upward respectively and the unit vectors in the direction of ox, oy, oz and $\boldsymbol{H}$ be $\boldsymbol{i}, \boldsymbol{j}, \boldsymbol{k}$ and $\boldsymbol{H}_0$ respectively and let $\boldsymbol{R}=\boldsymbol{j}\times\boldsymbol{H}_0$, dip of geomagnetic field be ϕ.

Let number densities of electrons, ions, +ions, −ions, be n_e, n_i, n_+, n_- respectively and let $n_-=\lambda n_e$, $n_+=(\lambda+1)n_e$, $n_i=(2\lambda+1)n_e=\kappa n_e$. (6)

In the following calculation it is assumed that the axis of rotation and the magnetism of the earth coincide, the following two cases (a) and (b) are considered.

(a) Only vertical component of the H.C. does not flow.

Here we discuss conductivity of the ionosphere in middle and low latitudes only.

(1) Conductivity of the ionosphere in the direction of E–W.

When an electromotive force (O, E_{0y}, O), parallel to the magnetic equator, is imposed, then vertical component of the H.C. produces an electric polarization, which produces an electric field E_z.

$\therefore$ $\boldsymbol{E}=(O, E_{oy}, E_z)$ Substituting this relation in (5) we get

$$\bar{\boldsymbol{C}}_1=\frac{e_1}{m_1}\left[\frac{\tau_1}{1+\omega_1^2\tau_1^2}\left\{(E_z\cos\phi+\omega_1\tau_1E_{0y})\boldsymbol{R}+(E_{0y}-\omega_1\tau_1E_z\cos\phi)\boldsymbol{j}\right\}-\tau_1E_z\sin\phi\cdot\boldsymbol{H}_0\right] \quad (7)$$

where 1 is either i or e.

Let $\bar{\boldsymbol{C}}_i=(U_i, V_i, W_i)$, $\bar{\boldsymbol{C}}_e=(U_e, V_e, W_e)$, then we have

$$W_i=e_i(p_iE_z+q_ie_y), \quad W_e=-e(p_eE_z+q_eE_y) \quad (8)$$

where $$p_i=\frac{1}{m_i\nu_i}\left(\frac{\nu_i^2}{\nu_i^2+\omega_i^2}\cos^2\phi+\sin^2\phi\right), \quad q_i=\frac{1}{m_i}\cdot\frac{\omega_i}{\nu_i^2+\omega_i^2}\cos\phi \quad (9)$$

and the same form holds for electrons. As here the vertical component of the H.C. does not flow, we have

$$-en_eW_e+e(\lambda+1)n_eW_+-e\lambda n_eW_-=0$$

Substituting (8) in the above equation, follows

$$E_z=\mu E_{0y}, \qquad \mu=-(q_1/p)\cos\phi$$

where $$p=p_e+\kappa p_i, \ q_1=(1/m)\{\omega_e/(\nu_e^2+\omega_e^2)\}+(1/m_i)\{\omega_+/(\nu_i^2+\omega_i^2)\} \quad (10)$$

Using these relations we have

$$\begin{cases}V_e=\left(-\dfrac{e}{m}\cdot\dfrac{\nu_e}{\nu_e^2+\omega_e^2}-\dfrac{1}{H}\cdot\dfrac{\omega_e^2}{\nu_e^2+\omega_e^2}\cdot\mu\cos\phi\right)E_{0y}\\ V_i=\left(\dfrac{e_i}{m_i}\cdot\dfrac{\nu_i}{\nu_i^2+\omega_i^2}-\dfrac{1}{H}\dfrac{\omega_i^2}{\nu_i^2+\omega_i^2}\cdot\mu\cos\phi\right)E_{0y}\end{cases}$$

therefore, the electric current in the E–W direction, I_y is,

$$I_y=Ze_jn_jV_j(j=e, +, -)$$
$$=\sigma_y\cdot E_{0y} \quad \text{where} \quad \sigma_y=n_e\cdot e^2\{p_1+(q_1^2/p)\cos^2\phi\} \quad (11)$$

$$p_{i1}=(1/m_i)\{\nu_i/(\nu_i^2+\omega_i^2)\} \text{ etc., } p_1=p_{e1}+\kappa p_{i1} \tag{12}$$

on the other hand the condnctivity by ions only is,

$$\sigma_{iy}\simeq e^2(\kappa n_e/m_i)\{\nu_i/(\nu_i^2+\omega_i^2)\} \tag{13}$$

(2) Conductivity of the ionosphere in the direction of *N–S*

Under the assumption that there is no vertical electric current, we have

$$\sigma_x=n_e\cdot e^2\cdot p_1p_0/(p_1\cdot\cos^2\phi+p_0\sin^2\phi) \tag{14}$$

where $p_{i0}=1/m_i\nu_i$, $p_0=p_{e0}+\kappa p_{i0}$ (15)

When an electro-motive force $\boldsymbol{E}=(E_x, E_y, O)$ is imposed, the electric current $\boldsymbol{I}=(I_x, I_y, O)$ is as follows

$$I_x=\sigma_x\cdot E_x+\sigma_{xy}\cdot E_y, \qquad I_y=\sigma_{yx}\cdot E_x+\sigma_y\cdot E_y \tag{16}$$

where $\sigma_{xy}=-\sigma_{yx}=-n_ee^2q_1\cdot\sin\phi$ (17)

is obtained in the same way.

(b) The H.C. does not flow in any direction.

(1) Conductivity of *E–W*

Let an electro-motive force be $\boldsymbol{E}_0=(O, E_{0y}, O)$ and $\boldsymbol{E}'=(E_x, O, E_z)$ be an electric field by polarization of the H.C., then $\boldsymbol{E}=(E_x, E_{0y}, E_z)$

Substituting this relation in (5), we get, for ions,

$$\bar{\boldsymbol{C}}_i=\frac{e_i}{m_i}\Big[\frac{\tau_i}{1+\omega_i^2\tau_i^2}\Big\{(-E_x\sin\phi+E_z\cos\phi+\omega_i\tau_iE_{0y})\boldsymbol{R}+(E_{0y}-\omega_i\tau_i(-E_x\sin\phi+E_z\cos\phi))\boldsymbol{j}\Big\}$$
$$-\tau_i(E_x\cos\phi+E_z\sin\phi)\boldsymbol{H}_0\Big]$$

then $W_i=e_i(s_iE_x+p_iE_z+q_iE_y)$, $U_i=e_i(r_iE_x+s_iE_z+u_iE_y)$ etc. (18)

As, here, both horizontal and vertical components of the H.C. do not flow,

$$\begin{cases}-en_eW_e+e(\lambda-1)n_eW_+-e\lambda n_eW_-=0\\ -en_eU_e+e(\lambda-1)n_eU_+-e\lambda n_eU_-=0\end{cases}$$

From these relations and (15) we have $E_x=\mu_xE_{0y}$, $E_z=\mu_zE_{0y}$

and so $V_i=\Big\{\frac{e_i}{m_i}\cdot\frac{\nu_i}{\nu_i^2+\omega_i^2}-\frac{1}{H}\frac{\omega_i^2}{\nu_i^2+\omega_i^2}(-\mu_x\sin\phi+\mu_z\cos\phi)\Big\}E_{0y}$

therefore $I_y=\Sigma e_jn_jV_j=\sigma_y\cdot E_{0y}$ where $\sigma_y=n_e\cdot e^2(p_1+q_1^2/p_1)$ (19)

(2) Conductivity of *N–S*

In the same way as above we have

$$\sigma_x=n_e\cdot e^2\cdot p_0(p_1^2+q_1^2)/\{(p_1^2+q_1^2)\cos^2\phi+p_1p_0\cdot\sin^2\phi\} \tag{20}$$

When an electro-motive force $\boldsymbol{E}=(E_x, E_y, O)$ is imposed, the electric current $\boldsymbol{I}=(I_x, I_y, O)$ is $I_x=\sigma_x\cdot E_x$, $I_y=\sigma_y\cdot E_y$

4. Consideration on the ratio of number densities of electrons and ions in the ionsphere.

To estimate λ, we must go into some details of the recombination and attachment processes. The equations between n, n_e, n_-, n_+, are as follows:

$$\begin{cases}dn_e/dt=I+\rho n_-+\delta n_-n_0-\beta n_an_e-\alpha n_en_+-\dfrac{n_e}{T}\dfrac{dT}{dt}\\ dn_-/dt=\beta n_an_e-\gamma n_-n_+-\rho n_--\delta n_-n_0-\dfrac{n_-}{T}\dfrac{dT}{dt}\end{cases}$$

where I=the number of electrons primarily produced in cm³/sec
α=the recombination coefficient for electrons in cm³/sec
β=the attachment coefficient for ions in cm³/sec
ρ=the coefficient of photo detachment in 1/sec
γ=the recombination coefficient for ions in cm³/sec
n_0=the number density of atomic oxygen
n_a=the number density of particles, for which electrons can attach, that is $n_a=n_0$ or $n_e=n_{02}$

From above equations, we have $n_-=\lambda n_e$

where $$\lambda=(\alpha n_e^2+\frac{n_e}{T}\frac{dT}{dt}+\frac{dn_e}{dt}+\beta n_e n_a-I)/(\delta n_e n_0+\rho n_e-\alpha n_e^2) \qquad (21)$$

According to Penndorf [4], the transition layer is situated near the height of $n=5\cdot10^{13}$. Oxygen is almost atomic in higher region than that, and almost molecular in the lower.

According to Bates and Massey [5] in the $F2$ and E layer, $\lambda=8\cdot10^{-5}$, $9\cdot10^{-2}$ respectively in the day time.

Below the transition layer, neglecting dT/dt, $d\lambda/dt$, from (21) we have

$$\lambda=\beta n_e\cdot n_a/(\rho n_e+\gamma n_e^2+q) \qquad (22)$$

where $q=I/(1+\lambda)$
$\rho=0.14$ (almost independent of the zenith angle of the sun)
$\gamma=10^{-7}\sim10^{-8}$
and $\beta=4.3\times10^{-13}\times e^{-z}+10^{-14}$ where z is height from 60 km level, measured in unit of 10^6 cm.

As q is not greater than 10^2, we can neglect q and therefore

$$\lambda=(4.3\times10^{-12}\times e^{-z}+10^{-13})n_{02}/1.4 \qquad (23)$$

From the above we get Table 1.

Table 1.

Region	n	λ	$\varkappa$
$F2$	4.10^{10}	$8\cdot10^{-3}$	1
E	6.10^{12}	$9\cdot10^{-2}$	1
D	10^{14}	$1\cdot10$	22
	10^{15}	$2.6\cdot10^{2}$	$5.2\cdot10^{2}$
	10^{16}	$6.14\cdot10^{3}$	$1.2\cdot10^{3}$

5. Results of numerical calculation.

Case (3, a, 1)

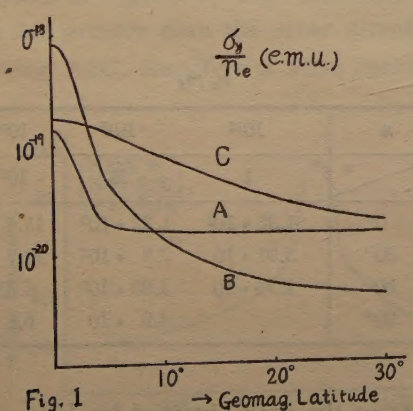

Fig. 1

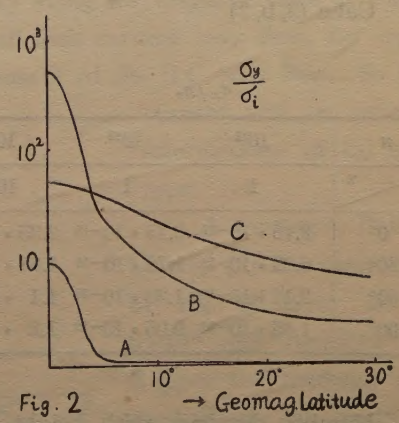

Fig. 2

We obtain results shown in Fig. 1 and 2, where A, B, C are shown in Table 2.

When $n \leqq 10^{11}$; $n = 10^{13}$, $\kappa > 10^2$, the effect of H.C. dissappears.

Table 2

	n	$\varkappa$
A	10^{12}	1
B	10^{13}	1
C	10^{13}	20

Case (3, a, 2)

Table 3

σ_x / n_e (emu)

n / ϕ \ $\varkappa$	10^{13}	10^{14}
	1	10^2
0°	$2.16 \cdot 10^{-18}$	$2.32 \cdot 10^{-19}$
10°	$9.7 \cdot 10^{-20}$	$1.94 \cdot 10^{-19}$
30°	$1.22 \cdot 10^{-20}$	$8.5 \cdot 10^{-20}$

σ_x / σ_i

n / ϕ \ $\varkappa$	10^{13}	10^{14}
	1	10^2
0°	$1.23 \cdot 10^3$	$1.32 \cdot 10$
10°	$5.5 \cdot 10$	$1.1 \cdot 10$
30°	1.9	4.83

σ_{xy} / n_e (indep of $\varkappa$)

ϕ \ n	10^{12}	10^{13}	10^{14}
0°	0	0	0
10°	$8.3 \cdot 10^{-21}$	$9.16 \cdot 10^{-21}$	$8.75 \cdot 10^{-21}$
30°	$2.38 \cdot 10^{-20}$	$2.63 \cdot 10^{-20}$	$2.51 \cdot 10^{-20}$

(ϕ is the dip of the geomagnetic field.)

Case (3, b, 1) σ_y / n_e is almost independent of ϕ.

Table 4

σ_y / n_e

n \ $\varkappa$	1	10^2
10^{11}	$1.46 \cdot 10^{-20}$	$1.44 \cdot 10^{-18}$
10^{12}	$1.58 \cdot 10^{-19}$	$1.61 \cdot 10^{-18}$
10^{13}	$9.1 \cdot 10^{-19}$	$1.92 \cdot 10^{-19}$
10^{14}	$2.17 \cdot 10^{-19}$	$1.14 \cdot 10^{-19}$

σ_y / σ_i

n \ $\varkappa$	1	10_2
10^{11}	1	1
10^{12}	9.9	1
10^{13}	$5.18 \cdot 10^2$	1.1
10^{14}	$1.23 \cdot 10^3$	6.5

Cabe (3, b, 2)

Table 5

σ_x / n_e

n / ϕ \ $\varkappa$	10^{12}	10^{13}	10^{14}
	1	1	10^2
0°	$2.15 \cdot 10^{-17}$	$2.15 \cdot 10^{-18}$	$2.35 \cdot 10^{-19}$
30°	$6.22 \cdot 10^{-19}$	$1.76 \cdot 10^{-18}$	$1.88 \cdot 10^{-19}$
60°	$2.12 \cdot 10^{-19}$	$1.32 \cdot 10^{-18}$	$1.1 \cdot 10^{-19}$
90°	$1.85 \cdot 10^{-19}$	$9.05 \cdot 10^{-19}$	$1.2 \cdot 10^{-19}$

σ_x / σ_i

n / ϕ \ $\varkappa$	10^{12}	10^{13}	10^{14}
	1	1	10^2
0°	$1.35 \cdot 10^3$	$1.22 \cdot 10^3$	13.4
30°	$3.91 \cdot 10$	$7.8 \cdot 10^2$	10.7
60°	$1.34 \cdot 10$	$2.93 \cdot 10^2$	6.35
90°		$4.9 \cdot 10$	6.8

Number densities with height calculated from the data obtained by $V2$ rocket [6] are shown in Table 6.

Table 6

Height (km.)	n
110	$2.41 \cdot 10^{12}$
100	$8.05 \cdot 10^{12}$
90	$6.98 \cdot 10^{13}$
80	$4.82 \cdot 10^{14}$
70	$2.05 \cdot 10^{15}$

Using these results, we calculated the conductivities of the E and $F2$ layers which have Chapman distribution, at midday at the equator. In the E and F layer, we assumed that at the level of maximum ionization, $n=6 \cdot 10^{12}$, $4.3 \cdot 10^{10}$ respectively and the temperature is 300°K, 1,000°K; local scale height is 10^6 cm, $5.42 \cdot 10^6$ cm respectively. Then the conductivity integrated with height is $1.6 \times 10^{-12} n_{e0}$ for the E layer and $1.33 \times 10^{-13} n_{e0}$ for the $F2$ layer, where n_{e0} is maximum electron density for each layer.

6. Examination of the result.

We examine the electrical conductivity of the ionosphere mainly concerning the diurnal variation of the terrestrial magnestism. At first we consider that electron density is everywhere constant at the same altitude.

As it is most probable that Sq-current flows mainly in the E layer or in and blow the E layer, the following two cases are considered.

(a) Only vertical component of the H.C. does not flow.

If $\kappa<50$ at the height of $n=10^{12}$, 10^{13}, and if $\kappa<100$ at the height of $n=10^{14}$, σ_y is considerably great near the magnetic equator and rapidly decreases at 10° of latitudes towards higher latitudes. According to the examination of the previous section, κ seems to be in these ranges, if κ is greater than these ranges, this tendency disappears. At low latitudes σ_{xy} is small compared with σ_y. Therefore, when an electromotive force, which is nearly parallel to the equator, as in Sq field near midday is imposed there, I_y is approximately determined by $I_y=\sigma_y \cdot E_{0y}$.

(b) The H.C. does not flow in any direction.

Below the height of $n=10^{12}$, σ is appreciably greater than σ_i, and σ_y is almost independent of latitude.

The horizontal component of the H.C. caused by the Sq current in the day time, will tend to concentrate negative charges to the centre C of the current vortex, as shown in Figure 4. But since the conductivity along the magnetic lines of force BC is far greater than the other directions, a small leak current may flow, for example along ABC, therefore a little horizontal component of the H.C. may flow. So the Sq current will be considered intermediate of (a) and (b) type.

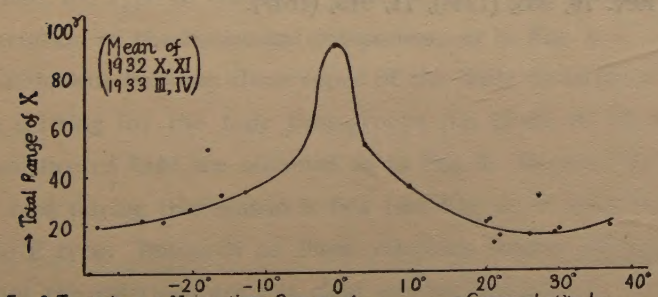

Fig. 3 Total diurnal Variation Range of North Comp. of Terr. Mag. with Geomag. Latitude

According to Bates and Massey [5] the mean density of the E layer is about $6 \cdot 10^{12}/cm^3$, therefore in the E layer the tendency of the conductivity at $n=10^{13}$ will sufficiently hold.

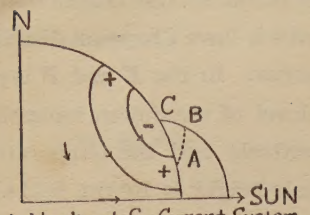

Fig.4 Idealized Sq Current System

According to the statistical research by Prof. M. Hasegawa and Dr. M. Ota, as shown in Fig. 3, there is a narrow region along the geomagnetic equator, about 20° of latitude wide, in which the range of the diurnal variation of terrestrial magnetism is much greater than in the other region. On the other hand radio exploration of the E layer seems to show that the electron density of the layer approximately follow Chapman distribution, therefore there is no particularly great electron density in the narrow region along the geomagnetic equator. When we try to explain this distribution of Sq by the dynamo theory, it seems very reasonable to consider that the mode of electric currents in the E layer or in its vicinity i.e. in the region of $10^{11}<n<10^{15}$, is between (a) and (b).

In the real ionosphere, near the level of the E layer, there will be a narrow region, along the magnetic equator at that level, in which the conductivity is much greator than in the other latitudes.

Moreover, it is considered appropriate that at least in the daytime κ is of order 1 near the level of $n=10^{13}$.

Acknowledgement

The writter wishes to express his thanks to Prof. M. Hasegawa for his constant interest and encouragement in this work, and to Dr. M. Ota and Dr. Y. Tamura for his advice in this work.

References

[1] S. Chapman and T.G. Cowling, 'The mathematical theory of non-uniform gases' 329 Cambridge, (1939).

[2] V.C.A. Ferraro, Terr. Mag. **50**, 215, (1945).

[3] T.G. Cowling, Mon. Not. Roy. Astro. Soc. **93**, 90, (1933).

[4] R. Penndorf, J. Geophys. Res. **54**, 7, (1949).

[5] D.R. Bates and H.S.W. Massey, Proc. R. Soc. A, **187**, 261, (1946).

[6] N. Best and others, Phys. Rev. **70**, 985, (1946), **71**, 915, (1847).

Circulatory Motions in the Ionospheric Atmosphere and their Relation to the S Field of the Terrestrial Magnetism. III

By Sadami MATSUSHITA

Geophysical Institute, Kyoto University

Abstract

The relations between the shifting of ionic clouds of the sporadic-E and the type of the daily variation of the terrestrial magnetism are discussed in more detail than in the first report. Moreover, a research is being made regarding the shifting of ionic clouds of the F2 layer.

From these results, it becomes necessary to consider the semi-diurnal variation of the ionosphere. Therefore, the semi-diurnal variation and its relation to the S field of the terrestrial magnetism are discussed. Also a research of the dynamo effect due to both the diurnal and the semi-diurnal variation is being conducted.

1. Further Discussion on Relations between the Shifting of Ionic Clouds of the Sporadic-E and the Type of the Daily Variation of the Terrestrial Magnetism

The relations between the shifting of ionic clouds of the sporadic-E (Es) and the type of the daily variation of the terrestrial magnetism have been discussed already in the first report, in which ionospheric data in Japan for June 1949 were studied mainly (1). In this report, a research conducted on these relations during June solstice and equinoxes of 1949, except days of non-observation, is discussed. At that time, the type of the daily variation of the terrestrial magnetism is classified by the variation of the horizontal component, as in Fig. 1.

Relations between these types of the daily variation at Kakioka and the direction of the shifting for the four time-groups (i.e. 01–07, 07–13, 13–19 and 19–01 h.) during June solstice of 1949 are obtained as in Fig. 2. Because the number of the days of the E type during this season is few (see Fig. 4), it is difficult to obtain these relations for the E type. Research on these relations during equinoxes of 1949 is conducted also, but the relations are not clear except the case of the storm time, since the Es in this season is not intense at the quiet time.

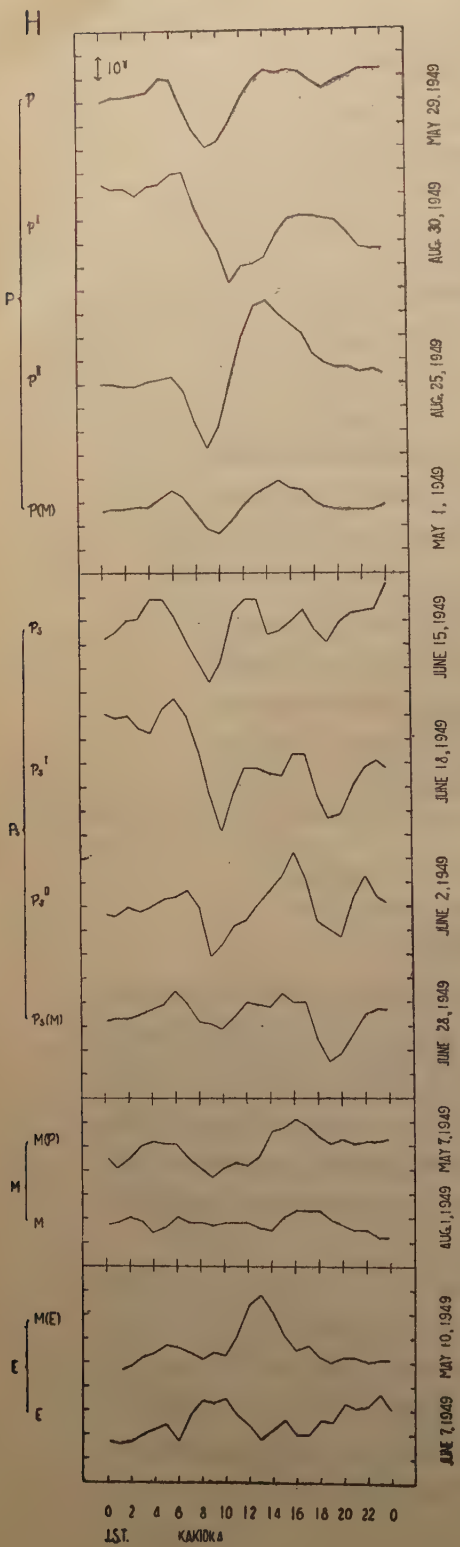

Fig. 1 Classification of the type of the daily variation of the terrestrial magnetism. p, M and E are owing to Hasegawa's classification (2). Other notations are as follows:

- p^{I} when maximum is in the forenoon.
- p^{II} when maximum is in the afternoon.
- p (M) when difference from maximum to minimum is small.
- M (p) when difference from maximum to minimum is smaller than p(M).
- M(E) when variation is small in the forenoon but increases in the afternoon.

Types with suffix s indicate some disturbed cases with somewhat intense decrease at night.

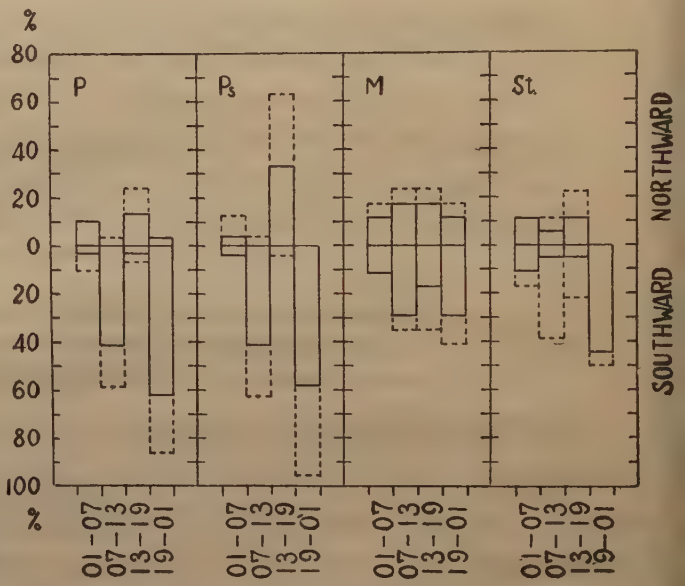

Fig. 2 Frequencies (in percentage) of the occurrence of the southward shifting (downward) and the northward shifting (upward) of the Es, in the cases of the P type (29 examples), the Ps type (24 examples), the M type (21 examples) of the daily variation and the storm time (18 examples) of the terrestrial magnetism, during June solstice of 1949. They are classified in four time-groups (01–07, 07–13, 13–19 and 19–01 h. of J.S.T.) and the dotted line shows cases when the shifting is not very conspicuous.

In Fig. 2, the relations between the shifting and the type, mentioned in the first report, are also obvious in this period. Namely, in the case of the P type and especially the Ps type, the change of direction of the shifting for the four time-groups is conspicuous, though it is obscure in the case of the M type and the storm time.

From the aspect of these changes of the direction of the shifting for the case of the P type, it becomes necessary to consider the semi-diurnal variation of the ionosphere. It will be discussed in paragraph three.

In addition, frequencies and the time for occurrence of the intense and sharp decrease of the value of the horizontal component of the terrestrial magnetism in the case of the Ps type adopted to this statistical study during June solstice and equinoxes of 1949 are shown in Fig. 3. It occurs most frequently at 19 h., and this may have some relation to the S_D field. The obvious southward shifting at night of the Ps type may be an evidence of the effect of the S_D field, beside the effect of the semi-diurnal variation. Fig. 4 is frequencies of occurrence of each type of the daily variation of the terrestrial magnetism, adopted to this statistical study during June solstice of 1949.

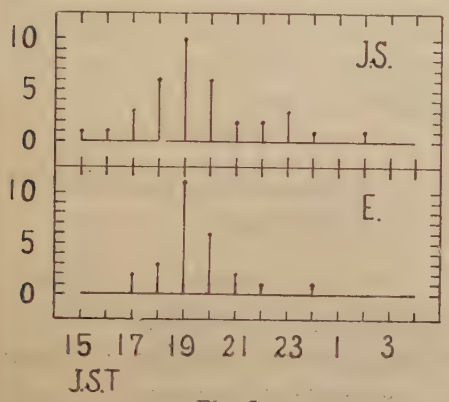

Fig. 3

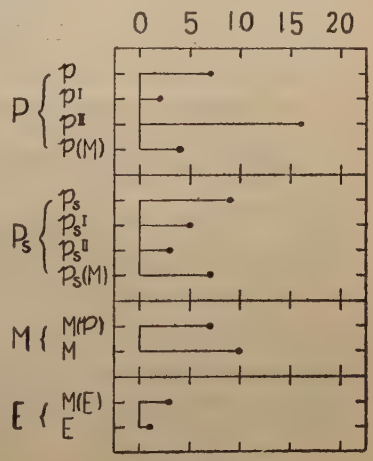

Fig. 4

The simultaneous variation of the Es region ionization in all observatories of Japan was discussed in the first report. Frequencies and the time of occurrence of the simultaneous variation during June solstice of 1949 are obtained as in Fig. 5. It is interesting to note from the figure that the simultaneous variation of the Es does not occur from 00 to 06 h. of J.S.T. but that it occurs most frequently at 08 h.. As the simultaneous variation seems to depend on the effect caused by particles from the sun, these results are suggestive to the character of the particles.

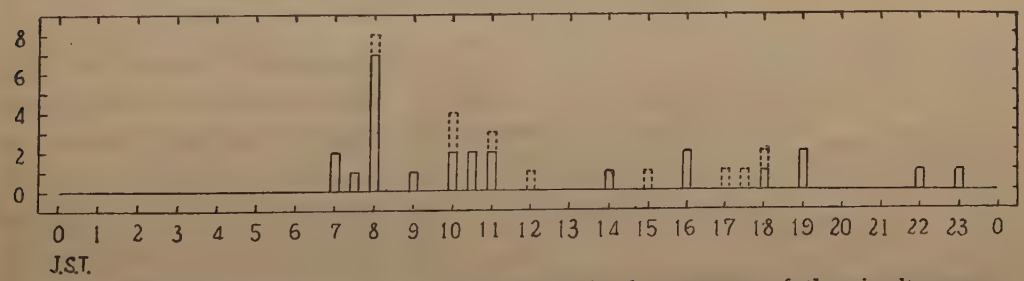

Fig. 5 Time (abscissa) and frequencies (ordinate) of occurrence of the simultaneous variation of the Es region ionization in Japan during June solstice of 1949. Squares are conspicuous cases of the simultaneous variation, and dotted-line-squares are the cases that are not so conspicuous.

Fig. 6 Frequencies (in percentage) of occurrence of the simultaneous variation of the Es region ionization in the four time-groups for each case of the P, the Ps and the M type of the daily variation and the storm time of the terrestrial magnetism during June solstice of 1949. Dotted line shows the cases when the variation is somewhat inconspicuous.
I : 01–07 h. II : 07–13 h.
III : 13–19 h. IV : 19–01 h.

Frequencies of occurrence of the simultaneous variation of the Es in the four time-groups for each type of the daily variation of the terrestrial magnetism are shown in Fig. 6. It is interesting, in the figure, that the simultaneous variation seems to occur frequently at the M type, and that the variation does not occur from the sun-set to the sun-rise, except the case of the storm time of the terrestrial magnetism.

2. *Shifting of Ionic Clouds of the F2 Layer*

When the variation of the critical frequency of the F2 layer ($f^{\circ}F_2$) is investigated, some increment of $f^{\circ}F_2$ at midnight, in spite of no change of the height, is noted. The time of such occurrence is from 19 to 03 h.. Burkard (3) called it 'sporadic-F layer'. When such variations at the five ionospheric observatories in Japan (see Fig. 1 in the first report) are compared, as in the case of the statistical study of the Es region ionization, some apparent shifting is obtained as shown in Fig. 7.

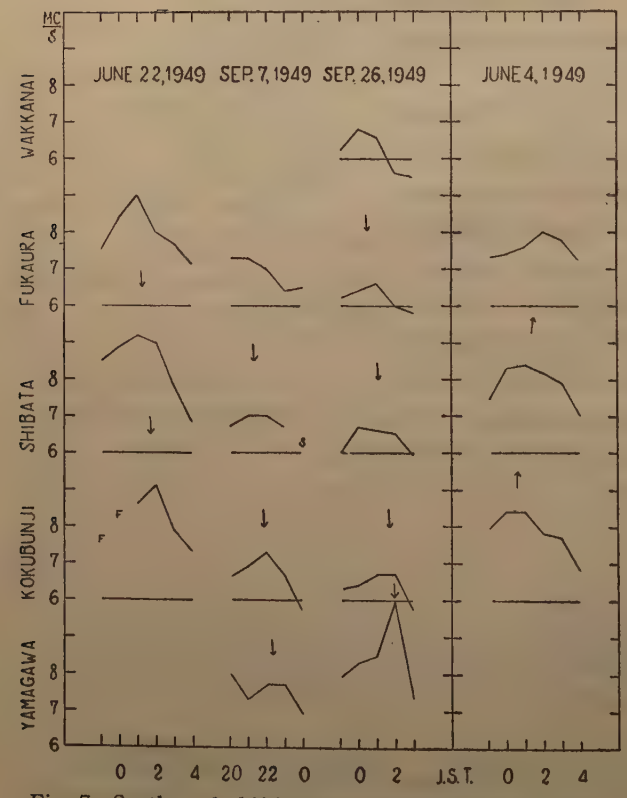

Fig. 7 Southward shifting (left) and northward shifting (right) of ionic clouds of the F2 layer.

It is difficult to explain this result by reason of the difference of sun-rise time and sun-set time at the five observatories. Because the direction of the shifting is both northward and southward in the same month. Accordingly, it may be possible to consider that ionic clouds of the F2 layer shift to the south

or the north, as in the case of ionic clouds of the Es region ionization. The time and frequencies of occurrence of such shifting in June solstice and equinoxes of 1949 are shown in Fig. 8.

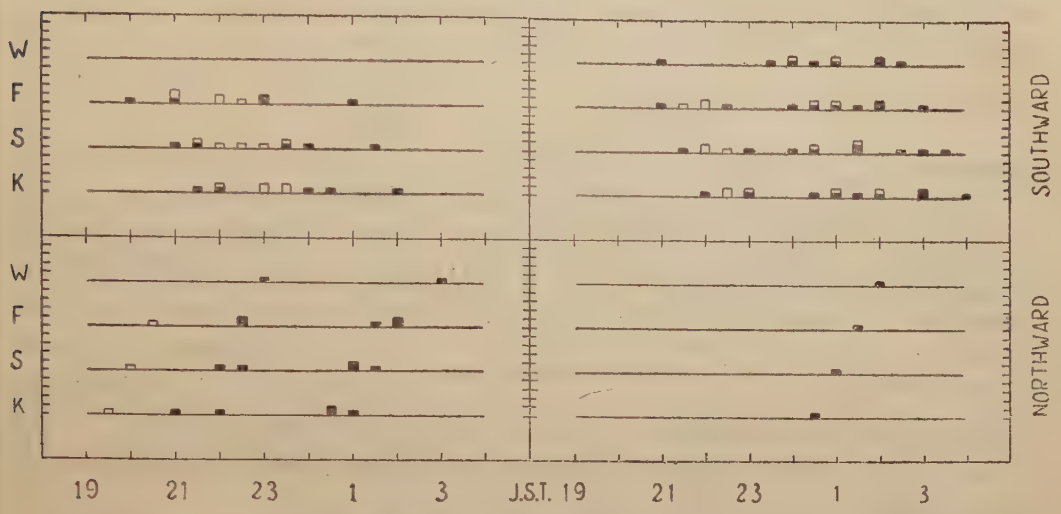

Fig. 8 Times (abscissa) and frequencies (ordinate) of occurrence of the southward shifting (the upper part) and the northward shifting (the lower part) of ionic clouds of the F2 layer at four observatories (Yamagawa is omitted, by the reason of few occurrence) in June solstice (left) and equinoxes (right) of 1949. The unit scale of ordinate is 2. Black squares are conspicuous cases of the shifting, and white squares are the cases that are somewhat inconspicuous.
W: Wakkanai, F: Fukaura, S: Shibata, K: Kokubunji.

The apparent velocity of the shifting is from 1080 to 360 km/h, and is 540 km/h as the mean of all. (cf. 370 km/h as the mean, in the case of the Es.) Most recently, the speed of sporadic clouds was obtained from the observation at Baker Lake by Meek (4). It was from 600 to 1300 km/h at the height from 250 to 300 km. He adopted 1200 km/h as the mean speed at the height of 300 km. It nearly corresponds to the abovementioned result, and speed 400 km/h obtained by him for the height of 100 km definitely corresponds to our result for the Es.

Frequencies of occurrence of the southward and the northward shifting of ionic clouds of the F2 layer for each type of the daily variation of the terrestrial magnetism during June solstice and equinoxes of 1949 are as follows:

Type	Southward Shifting				Northward Shifting			
	19–01 h.		01–03 h.		19–01 h.		01–03 h.	
	June Solstice	Equinoxes	June Solstice	Equinoxes	June Solstice	Equinoxes	June Solstice	Equinoxes
P	3(?)	4(2?)	1	2(1?)	1(?)	0	1	0
Ps	2(1?)	1(?)	0	2(1?)	0	0	0	1
M	0	0	0	0	0	0	0	0
E	1(?)	0	0	0	1	0	0	0
Storm	3	1	0	4	1	0	2	0

Numbers with question marks show frequencies for the cases when the shifting is not so obvious. As the examples are quite few, it is difficult to obtain accurate conclusions from this result. However, the southward shifting tends to occur at night for the P and Ps type. It resembles the case of the Es. Further, during storm time, the shifting —both the southward and the northward—occurs somewhat clearly, and in the case of the M type it does not occur at all.

Es Region	F2 Layer			
	S. Shifting		N. Shifting	
	June Solstice	Equinoxes	June Solstice	Equinoxes
S. Shifting	4(3?)	3	1(?)	0
N. Shifting	1	0	1	0
Simultaneous	3(2?)	0	0	0
Not Occur	2(1?)	11(5?)	4	1

When the southward or northward shifting of ionic clouds of the F2 layer occurs, frequencies of correspondence between the shifting of the F2 layer and that of the Es region in the same night are shown in the left table. Though the cases are quite few in this table, it seems the southward shifting in the F2 layer corresponds the sameward shifting in the Es region, when the shifting occurs in both regions.

3. On the Semi-Diurnal Variation

In the second report (1), the diurnal variation of the ionosphere due to circulatory motions was discussed and the dynamo action owing to the variation was calculated. But, from the aspect of the abovementioned change of the direction of the shifting of ionic clouds of the Es for the case of the P type of the daily variation of the terrestrial magnetism, it becomes necessary to consider the semi-diurnal variation of the ionosphere.

From ionospheric data obtained from various locations (see, Fig. 1 in the second report), the semi-diurnal variation of the virtual height of the F2 layer is analyzed, as in the case of the research for the diurnal variation.

Fig. 9 indicates the meridional distribution of both the semi-amplitude of the semi-diurnal variation of the virtual height of the F2 layer and the phase in hours, at which maximum of the variation occurs, in Mar., June and Sep. 1947. In this case also, as in the diurnal variation, the meridional distribution of the amplitude would be represented by the form of $C+DP_6^2$ (Schmidt's spherical function). Values of C and D for the months of Mar., June and Sep. 1947 are as follows:

	March	June (only in the northern hemisphere)	September
C	20 Km	28 Km	26 Km
D	27 Km	27 Km	30 Km

The difference of the value between equinox and solstice is small, though there was great difference in the case of the diurnal variation (see dotted curves in Fig. 9). This suggests that the semi-diurnal variation does not directly depend on thermal effect.

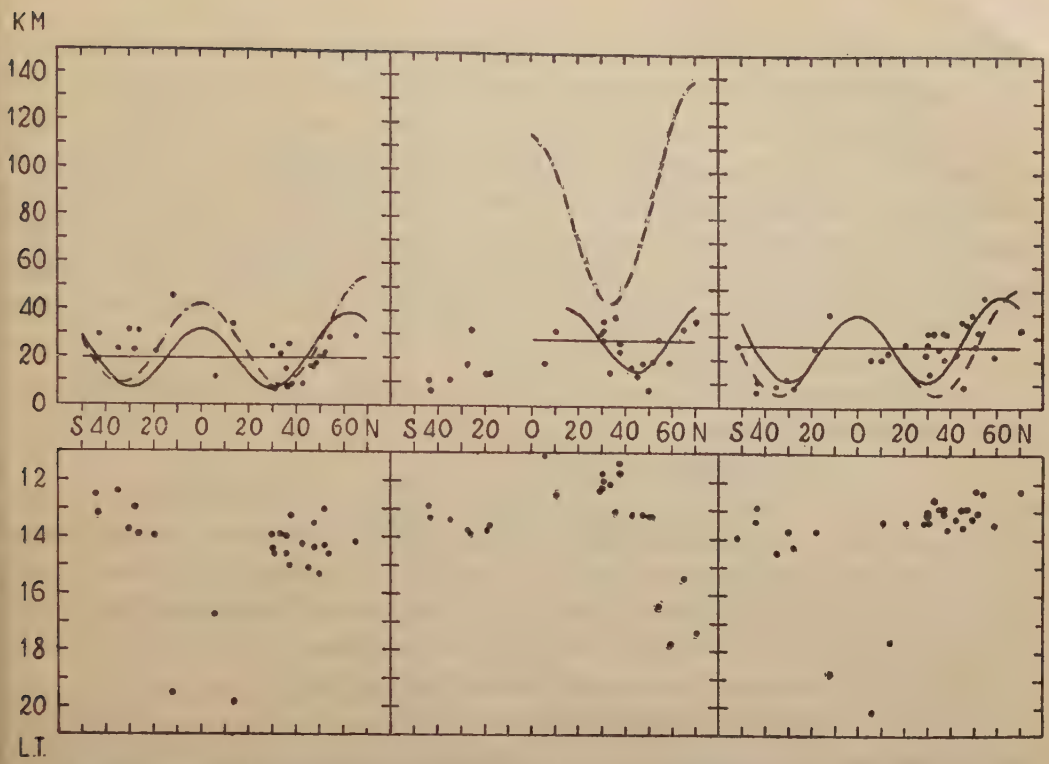

Fig. 9 upper part: Meridional distribution of the semi-amplitude of the semi-diurnal variation of the virtual height of the F2 layer in Mar. (left), June (middle) and Sep. (right) 1947. The horizontal lines indicate C, and the curves are $C+DP_6^2$. (The curve in June is treated only in the northern hemisphere and it is transfered 15° to the north from the form of $C+DP_6^2$.) Dotted curves are $A+BP_5^1$ of the diurnal variation (see the second report).
lower part: The phase in hours, at which maximum of the semi-diurnal variation of the virtual height of the F2 layer occurs, in Mar. (left), June (middle) and Sep. (right) 1947.
Abscissa: geographical latitudes

And the amplitude of the semi-diurnal variation for equinox is nearly of the same order as compared to that of the diurnal variation. But the amplitude of the diurnal variation for June in the northern hemisphere is about three times larger than that of the semi-diurnal variation, as the mean. Accordingly, in equinoxes and in middle latitudes of the northern hemisphere in June solstice, the semi-diurnal variation must be given important consideration. This is favourable to the foregoing results of the shifting of the ionic clouds.

In middle latitudes, the phase in hours is nearly same (about 13 h.) both in equinox and in solstice (see Fig. 9), though it has great difference in the case of the diurnal variation. From these results and from the point of view of the cause of the semi-diurnal variation in the upper atmosphere (5) (6), this variation may be caused by a tidal motion. But the form of this tidal motion will not be such a simple form as P_2^2, but may be the form of P_6^2 or the combined form of P_6^2 and P_4^2.

If it will be possible to assume that the phase for the semi-diurnal tidal variation

of the height of a layer lower than the E layer (for example, the D layer or the lower part of the E layer) has such a phase difference of 180°, as compared to that of the E and the F layer, as in the assumption for the circulatory motions, and that the form of the semi-diurnal tidal variation in the lower layer is represented by the form of $P_6^2-3P_4^2$, then it will be calculated by the dynamo theory (7), that the lower layer may produce Sq in spite of small electric conductivity, when the wind velocity of the layer is of order 100 m/s in middle latitudes, as in the case of the shifting of ionic clouds of the sporadic E region, and when the variation of the height is assumed to be the vertical rise and fall of an isobaric surface.

If the relative pressure oscillation for the semi-diurnal tidal circulation in the lower layer is assumed to be

$$0.15\ (P_6^2-3P_4^2)\sin(2t+60°),$$

there is a source of the air flow in the middle latitudes of the lower layer at 10 h. of the local time. The phase angle 60°—from this the abovementioned 10 h. is obtained —is determined by the assumption that the semi-diurnal variation in the lower layer has a minimum at 13 h., from the results that the semi-diurnal variation of the height of the F2 layer in middle latitudes has a maximum at about 13 h. as in Fig. 9.

From the assumption, the velocity potential is

$$1.28\times10^{12}\ (P_6^2-3P_4^2)\sin(2t-30°).$$

Fig. 10 indicates the air-velocities for this velocity potential. In the E and F layers, the direction of the wind is reverse to it in this figure. Accordingly, the direction of the wind in the E and F layers at the north of the source or the sink of the air-flow corresponds to the statistical results of the shifting of ionic clouds of the Es.

When the electric conductivity K is constant, the current function may be

$$(0.38\,P_7^2-0.61\,P_5^2-1.23\,P_3^2)\times10^{12}K\sin(2t-30°).$$

If the total electric current for this current function is of order 62,000 amp., such value of K is 5.0×10^{-9} e.m.u.,
and the electric current is shown in the right part of Fig. 10.

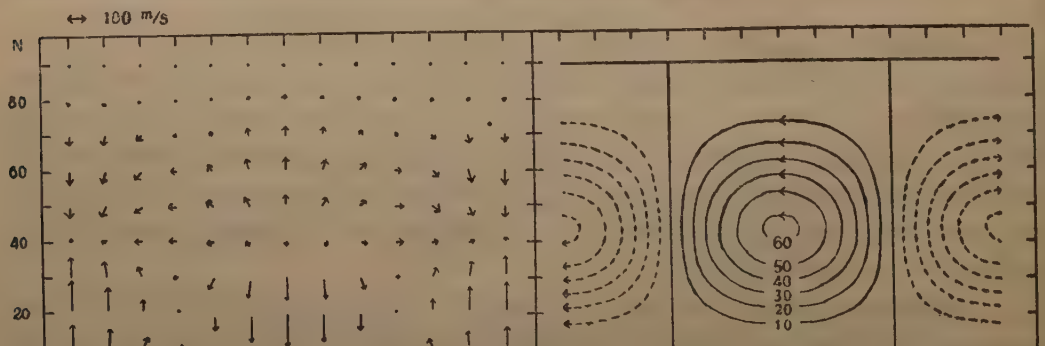

Fig. 10 The air-velocities in the layer for Sq (left) and the electric currents (right)—unit, 1,000 amp.—associated with the solar semi-diurnal tidal circulation of the form of $P_6^2-3P_4^2$ (shown for part of the northern hemisphere)
Abscissa: local time

In this case, the electric conductivity is calculated with the conception for only one current-seat, and so it will be necessary to consider the effect of the reverse electric current in the upper layer. If the electric conductivity of the layer for Sq is of order 10^{-8} e.m.u., assuming the wind velocity in middle latitudes of the layer is about 100 m/s (when the electric conductivity of the layer is much more, it will be sufficient with smaller wind velocity) and assuming the electric conductivity of the F2 layer is of order 10^{-9} e.m.u. (6), then the lower layer will produce the Sq field sufficiently, under the conception of the effect of two current-seats.

4. The S Field due to both the Diurnal and the Semi-Diurnal Variation of the Ionosphere

The diurnal variation of the ionosphere due to circulatory motions and the semi-diurnal variation owing to the tidal circulation have been considered separately, and the dynamo action have been calculated respectively. Now the dynamo action due to both the diurnal and the semi-diurnal variation will become necessary to consider.

From the comparison of the amplitude of the diurnal and the semi-diurnal variation of the ionosphere, it may be estimated as the mean state of a year that the dynamo effect due to the semi-diurnal variation is 0.6 times larger than that due to the diurnal variation. Because, from the abovementioned results that the amplitude of the diurnal variation of the F2 layer is three times larger* than that of the semi-diurnal variation in June solstice, but both are nearly equal in Dec. solstice and equinoxes, the ratio of the amplitude of the diurnal variation to that of the semi-diurnal variation as the mean state of a year is 5 : 3, i.e. 1 : 0.6. Accordingly, the Sq field due to the two variations is calculable by the assumption that the foregoing dynamo effect for each variation contributes respectively to the production of Sq with such a dynamo effect as this ratio.

Fig. 11 is the electric currents obtained from these estimations, when the electric conductivity at this time is about one-half of the conductivity in the case of the calculation of the electric currents for either one variation. It resembles generally to the electric currents obtained from geomagnetical data (7) (8).

---

* In Japan, the amplitude of the diurnal variation in June solstice is not always larger than that of the semi-diurnal variation. It corresponds with the semi-diurnal change of the direction of the shifting of ionic clouds of the Es. But in geomagnetically high latitudes, the amplitude of the diurnal variation in June solstice is very larger than that of the semi-diurnal variation. This will be discussed in near future.

Fig. 11 The electric currents—unit, 1,000 amp.—associated with both the diurnal circulatory motions and the semi-diurnal tidal circulation. (shown for the northern hemisphere)

In the case of the S_D field too, both the diurnal and the semi-diurnal variation must be considered. The principle for the calculation is already mentioned in the second report.

5. Whole Conclusions for Three Reports

The shifting of ionic clouds in the Es region and the F2 layer was discussed, using the data from the five ionospheric observatories in Japan. Though the eastward and westward shifting was difficult to obtain as the observatories were situated on almost the same meridian, the southward and northward shifting was certain. The speed of the shifting and the relations between the type of the daily variation of the terrestrial magnetism and the shifting of ionic clouds were obtained. The semi-diurnal change of the direction of the shifting in the case of the P type and the Ps type during June solstice was conspicuous.

On the other hand, a research on meridional distribution of the virtual height of the ionosphere for the daily mean was conducted, and general circulation in the ionospheric atmosphere was estimated.

Moreover, the diurnal variation and the semi-diurnal variation of the F2 layer

were analyzed in each season, and the meridional distributions of their amplitudes and phases were studied, using the data of the virtual height from many ionospheric observatories over the world. From these results, it may be most possible to consider that the diurnal variation depends on circulatory motions owing to thermal expansion and that the semi-diurnal variation depends on tidal circulations.

These assumptions may be convenient to explain a cause of the production of the S field of the terrestrial magnetism. Namely, if a layer lower than the E layer (for example, the D layer or the lower part of the E layer) has such wind that the direction is reverse to the wind supposed from both the shifting of ionic clouds in the Es region and the F2 layer and variations of the height of the ionosphere, then the lower layer may produce the Sq field and the E-F layer may produce the S_D field, in spite of their small electric conductivity (of order 10^{-8} e.m.u. in the lower layer, when the wind speed is of order 100 m/s), as the difference of the dynamo effect for two layers.

Conclusively, a cause of the S field of the terrestrial magnetism was studied in some degree from the motions of the ionosphere, though these discussions were not always complete.

In conclusion, the writer wishes to express his hearty thanks to Prof. M. Hasegawa, Dr. T. Nagata, Dr. M. Ota and Mr. Y. Nakata for their many valuable advices and encouragement throughout this study, and also to Miss M. Kato and Miss M. Kanayama for their assistance in numerical computations.

(Read: May 25, 1950)

References

(1) S. Matsushita, Journ. Geomag. Geoelect., **1**, 35, 41 (1949).
(2) M. Hasegawa, Proc. Imp. Acad. Tokyo, **12**, 88 (1936).
(3) O. Burkard, Terr. Mng., **53**, 63 (1948).
(4) J.H. Meek, Terr. Mag., **54**, 339 (1949).
(5) C.L. Pekeris, Proc. Roy. Soc. Lond., A. **158**, 650 (1937).
(6) S. Matsushita, Journ. Geomag. Geoelect., **1**, 17 (1949).
(7) S. Chapman and J. Bartels, Geomagnetism, Oxford, 1940.
(8) M. Hasegawa and M. Ota, Rep. Intern. Assoc. Terr. Mag. Elect., Oslo Assemb., Aug. 1948.

Magnetic Anomalies and the Corresponding Magnetic Centres. I

By Tsuneji RIKITAKE

Earthquake Research Institute

Abstract

The writer proposed a method for finding the position, intensity and direction of a underground magnetic dipole from the corresponding magnetic anomaly on the earth's surface. In the first place, the distribution of the vertical force is expressed as follows;

$$Z=\sum_j\sum_k\binom{j}{k}\frac{\partial^j Z_{00}}{\partial x^{j-k}\partial y^k}x^{j-k}y^k.$$

With the aid of some relations concerning spherical harmonic functions, then, the coefficients of the spherical harmonic expansion of the magnetic potential on a sphere that entirely contains the magnetic matter are determined. The radius of the sphere which is included in the expression as a parameter adjusted so as to make the higher degree terms minimum in the next place.

Applying the method to the magnetic changes which accompanied the eruption of Miyakezima Island of 1940, a reasonable conclusion is obtained.

1. Introduction. Though it is not possible to determine uniquely the subterranean mass distribution to which the magnetic anomalies on the earth's surface are due, some methods have been proposed by a number of investigators for finding the mass distribution directly from the intensity distribution of the magnetic field on the surface. Under the assumption that the mass is concentrated on a certain subterranean plane, T. Nagata[1] showed a method by which the mass distribution was directly determined from the magnetic anomalies in any component of the magnetic field, dip or declination. Being slightly modified, the method is also applicable for the anomalies due to dykes. E.H. Vestine and N. Davids[2] proposed an interesting method for estimating the depth of magnetic matter. The method is based on the fact that sources of magnetic matter correspond mathematically to singularities of the magnetic field-components. Applying the method to an idealized case, they succeeded to obtain the depth of a subterranean magnetic pole.

In this paper, the writer investigates a method for finding the position, intensity and direction of a underground magnetic dipole from the corresponding magnetic anomaly on the earth's surface. As studied in the measurement of natural remanent

magnetism of igneous rocks,[3] the first degree terms in the spherical harmonic expansion of the magnetic potential are so large that the higher degree terms can be neglected in spite of complex arbitrary forms of rock specimens. Hence, it is easily presumed that the dipole terms are most important in the magnetic anomalies due to magnetic matter of which shapes do not deviate markedly from the sphere. Accordingly, the method will be applicable for any magnetic anomalies so far as the said condition is satisfied. Applying the method to actual anomalies, it will be able to determine the depth of the magnetic centres that roughly agree with the centres of the magnetic matter to which the anomalies are due.

2. Theory. We consider a sphere which is sufficiently large so that it contains entirely the magnetic matter considered. Denoting the radius of the sphere by a, the magnetic potential is given by

$$W=a\sum_{n=1}^{\infty}\sum_{m=0}^{n}(a/r)^{n+1}P_{nm}(a_n^m\cos m\phi+b_n^m\sin m\phi)\quad(r>a) \tag{1}$$

where P_{nm} denotes Neumann's spherical surface harmonics. Taking a coordinate of which origin coincides with the centre of the sphere, where $\theta=0$ axis agrees with z axis, and using the relations[4]

$$\left.\begin{aligned} r^{-n-1}P_{nm}\cos m\phi&=\frac{(-i)^m n!}{2\pi(n-m)!}\int_{-\pi}^{\pi}(z+ix\cos u+iy\sin u)^{-n-1}\cos mu\,du,\\ r^{-n-1}P_{nm}\sin m\phi&=\frac{(-i)^m n!}{2\pi(n-m)!}\int_{-\pi}^{\pi}(z+ix\cos u+iy\sin u)^{-n-1}\sin mu\,du,\end{aligned}\right\} \tag{2}$$

the typical term of (1) can be written as

$$W_n^m=\frac{(-i)^m}{2\pi}\frac{n!}{(n-m)!}a^{n+2}\int_{-\pi}^{\pi}(z+ix\cos u+iy\sin n)^{-n-1}(a_n^m\cos mu+b_n^m\sin u)du.$$

On differentiating with respect to z, the vertical component of the magnetic field is given by

$$Z=\frac{1}{2\pi}\sum_n\sum_m(-i)^m\frac{(n+1)!}{(n-m)!}a^{n+2}\int_{-\pi}^{\pi}(z+ix\cos u+iy\sin u)^{-n-2}(a_n^m\cos u+b_n^m\cos mu)du. \tag{3}$$

Further, differentiating $j-k$ and k times with respect to x and y, we get

$$\frac{\partial^j Z}{\partial x^{j-k}\partial y^k}=\frac{1}{2\pi}\sum_n\sum_m(-i)^{m+j}\frac{(n+j+1)!}{(n+m)!}a^{n+2}\int_{-\pi}^{\pi}\cos^{j-k}u\sin^k u(z+ix\cos u+iy\sin u)^{-n-j-z}\times$$
$$\times(a_n^m\cos mu+b_n^m\sin mu)du.$$

Putting x and y are both equal to 0, then, we have

$$\frac{\partial^j Z_{00}}{\partial x^{j-k}\partial y^k}=\frac{1}{2\pi}\sum_n\sum_m(-i)^{m+j}\frac{(n+j+1)!}{(n-m)!}a^{n+2}z^{-n-j-2}(a_n^m f_{jk}^m+b_n^m g_{jk}^m), \tag{4}$$

where

$$\left.\begin{matrix}f_{jk}^m\\ g_{jk}^m\end{matrix}\right\}=\int_{-\pi}^{\pi}\cos^{j-k}u\sin^k u\left.\begin{matrix}\cos\\ \sin\end{matrix}\right\}mu\,du. \tag{5}$$

f_{jk}^m and g_{jk}^m are calculated for the cases j, k, $\leqq 3$ and $m\leqq 2$ as given in Table I.

Table I

f \ m	0	1	2	g \ m	0	1	2
f_{00}^m	2π	0	0	g_{00}^m	0	0	0
f_{10}^m	0	π	0	g_{10}^m	0	0	0
f_{11}^m	0	0	0	g_{11}^m	0	π	0
f_{20}^m	π	0	$\frac{\pi}{2}$	g_{20}^m	0	0	0
f_{21}^m	0	0	0	g_{21}^m	0	0	$\frac{\pi}{2}$
f_{22}^m	π	0	$-\frac{\pi}{2}$	g_{22}^m	0	0	0
f_{30}^m	0	$\frac{3}{4}\pi$	0	g_{30}^m	0	0	0
f_{31}^m	0	0	0	g_{31}^m	0	$\frac{\pi}{4}$	0
f_{32}^m	0	$\frac{\pi}{4}$	0	g_{32}^m	0	0	0
f_{33}^m	0	0	0	g_{33}^m	0	$\frac{3}{4}\pi$	0

On the other hand, we can obtain $\frac{\partial^j Z_{00}}{\partial x^{j-k}\partial y^k}$ from the observation or the observed distribution of the vertical intensity is expressed by

$$Z=\sum_j\sum_k\binom{j}{k}\frac{\partial^j Z_{00}}{\partial x^{j-k}\partial y^k}x^{j-k}y_k.$$

In case of $j,\ k\leqq 3$ and $n\leqq 2$, (4) gives the next simultaneous equations for the coefficients of the spherical harmonic expansion.

$$\left.\begin{aligned}
2a_1^0+3a_2^0&=Z_{00}\,,\\
3a_1^1+4\sqrt{3}\,a_2^1&=-a\partial Z_{00}/\partial x,\\
3b_1^1+4\sqrt{3}\,b_2^1&=-a\partial Z_{00}/\partial y,\\
12a_1^0+30a_2^0-5\sqrt{3}\,a_2^2&=-a^2\partial^2 Z_{00}/\partial x^2,\\
5\sqrt{3}\,b_2^2&=-a^2\partial^2 Z_{00}/\partial x\partial y,\\
12a_1^0+30a_2^0+5\sqrt{3}\,a_2^2&=-a^2\partial^2 Z_{00}/\partial y^2,\\
45a_1^1+90\sqrt{3}\,a_2^1&=-a^3\partial^3 Z_{00}/\partial x^3,\\
15b_1^1+30\sqrt{3}\,b_2^1&=-a^3\partial^3 Z_{00}/\partial x^2\partial y,\\
15a_1^1+30\sqrt{3}\,a_2^1&=-a^3\partial^3 Z_{00}/\partial x\partial y^2,\\
45b_1^1+90\sqrt{3}\,b_2^1&=-a^3\partial^3 Z_{00}/\partial y^3,
\end{aligned}\right\}\qquad(6)$$

where it is assumed that $z=a$. $a_1^0, a_1^1, b_1^1,\ldots$ are taken to be convenient for Schmidt's spherical surface harmonics.

As studied in connexion with the eccentric dipole for the earth's main field,[5),6)] the magnetic centre should be chosen so as to make $(a_2^0)^2+(a_2^1)^2+(b_2^1)^2+(a_2^2)^2+(b_2^2)^2$ minimum. This condition is satisfied when the centre is situated at

$$\left.\begin{aligned}
&x_0=a(L_0-a_1^0E)/3H_0^2,\quad y_0=a(L_1-a_1^1E)/3H_0^2,\quad z_0=a(L_2-b_1^1E)/3H_0^2,\\
&\text{where}\\
&H_0^2=a_1^0a_1^0+a_1^1a_1^1+b_1^1b_1^1\quad,\\
&L_0=2a_1^0a_2^0+(a_1^1a_2^1+b_1^1b_1^1)\sqrt{3}\quad,
\end{aligned}\right\}\qquad(7)$$

$$L_1=-a_1^1a_2^0+(a_1^0a_2^1+a_1^1a_2^2+b_1^1b_2^2)\sqrt{3}\ ,$$
$$L_2=-b_1^1a_2^0+(a_1^0b_2^1-b_1^1a_2^2+a_1^1b_2^2)\sqrt{3}\ ,$$
$$E=(L_0a_1^0+L_1a_1^1+L_2b_1^1)/4H_0^2\ .$$

Adjusting a or z so as to make $z_0=0$, we can determine the parameter a or z. The depth of the magnetic centre is thus obtained. Further, with the aid of (7), the position, intensity, and the direction of the dipole can be calculated.

In practice, the coefficients are determined by solving (6), while a remains as a parameter. The quantities included in (7) are calculated with these coefficients for various values of the parameter. The parameter must be determined by means of trial and error method so as to make $z_0=0$.

3. Test of the method. In order to test the method, a simple case is studied as follows. In the case of the anomaly in the vertical intensity due to a magnetic dipole, which is burried at a depth of D and directs downwards, we have

$$Z_{00}=2/D^3,\ \partial^2Z_{00}/\partial x^2=\partial^2Z_{00}/\partial y^2=-12/D^5,$$
$$\partial Z_{00}/\partial x=\partial Z_{00}/\partial y=\partial^2Z_{00}/\partial x\partial y=\partial^3Z_{00}/\partial x^3=\partial^3Z_{00}/\partial x^2\partial y=\partial^3Z_{00}/\partial x\partial y^2=\partial^3Z_{00}/\partial y^3=0,$$

where the moment of the dipole is taken to be unity.

In that case, the solutions of (6) become

$$a_1^0=\frac{1}{2D^3}\left(5-\frac{3a^2}{D^2}\right),\quad a_2^0=\frac{1}{D^3}\left(\frac{a^2}{D^2}-1\right),$$
$$a_1^1=a_2^1=a_2^2=b_1^1=b_2^1=b_2^2=0.$$

Then it is obvious that the potential due to the second degree terms becomes minimum by taking $a-D$. Thus, as assumed before, the anomaly is interpreted as that due to a magnetic dipole situated at the depth of D. As $a_1^0=1/D^3$ and $a_1^1=b_1^1=0$, it is also proved that the moment must be equal to unity and the direction is downward.

4. Actual example. As an actual example, the writer analyzed the magnetic changes that accompanied the eruption of Miyakezima Island in July, 1940. R. Takahasi and K. Hirano[7),8)] measured the changes in the vertical intensity during the period from July 20 to 29. From the repeated observations at 50 stations, they showed the distribution of the changes as reproduced in Fig. 1.

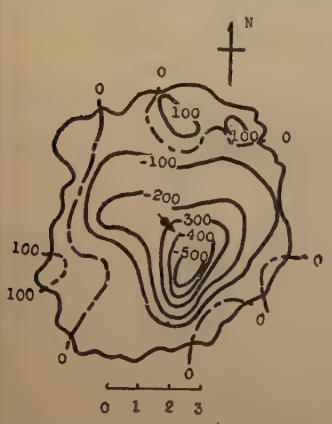

The changes in the vertical force that accompanied the eruption of Volcano Miyakejima. Unit ; γ (After R. Takahasi and K. Hirano)

The writer, in the first place, expressed the distribution in the form

$$Z=A+Bx+Cy+Dx^2+Exy+Fy^2+Gx^3+Hx^2y+Ixy^2+Jy^3,$$

where the origin was suitably taken at the centre of the island. The values of Z at intersection points of series of parallel lines which were drawn on the figure at about 1.2 km interval were read off. Using these values, the constants A, B, C,....were determined by means of least square. From these constants, Z_{00}, $\partial Z_{00}/\partial x$, $\partial Z_{00}/\partial y$, ...were calculated. Then, solving (6), a_1^0, a_1^1, b_1^1,.... were obtained. The value of a that makes $z_0=0$ was

calculated by means of trial and error method, being determined to be 2.9 km. Meanwhile, Takahasi and Hirano concluded that the changes were equivalent to those which might occur if a sphere, of which centre was situated at the depth of 3 km, lossed its magnetic susceptibility. Hence, the present result agreed well with their study. Further, it was found that the obtained direction and intensity of the dipole also supported their conclusions. The position of the dipole thus obtained was marked on the map with a small circle.

5. Conclusions. The writer studied a method for finding the depth, direction, and intensity of an underground magnetic dipole from the anomaly in the vertical intensity observed at the earth's surface. Taking into consideration that the dipole terms should be the most predominant in the anomaly due to magnetic matter, of which shape does not deviate markedly from the sphere, the method may be applicable for analyzing actual anomalies. The position of magnetic centre thus obtained will be roughly agree with the centre of magnetic matter which causes the anomaly.

In conclusion, the writer wishes to express his cordial appreciations to Dr. T. Nagata for his kind criticisms.

(Read: May 22, 1950)

References

1) T. Nagata, Bull. Earthq. Res. Inst. **16**, 550 (1938).
2) E.H. Vestine and N. Davids, Terr. Magn. **50**, 1 (1945).
3) T. Nagata, Bull. Earthq. Res. Inst. **21**, 1 (1943).
4) E.W. Hobson, The Theory of Spherical and Ellipsoidal Harmonics. pp. 99 and 103.
5) Ad. Schmidt, Gerl. Beitr. z. Geophys. **41**, 346 (1943).
6) J. Bartels, Terr. Magn. **41**, 225 (1936).
7) R. Takahasi and K. Hirano, Bull. Earthq. Res. Inst. **19**, 82 (1941).
8) R. Takahasi and K. Hirano, Bull. Earthq. Res. Inst. **19**, 373 (1941).

Magnetic Anomalies and the Corresponding Magnetic Centres. II

By Tsuneji RIKITAKE

Earthquake Research Institute

Abstract

The method described in the first report is extended to cases in which magnetic anomalies are given in dip.

The changes in magnetic dip that accompanied the Shizuoka Earthquake of 1935 are studied as an example.

1. Introduction. In the first report[1] of this paper, the writer proposed a method by which the position of magnetic centres of magnetic anomalies were directly determined from the observation of the vertical intensity of magnetic field on the earth's surface. The method will be extended here to cases in which magnetic anomalies are given in dip.

2. Magnetic anomalies in X and Y. In a similar way with the treatment of anomalies in Z, the partial derivatives of X and Y (the northward and eastward components) at $x=y=0$ are calculated as follows;

$$\frac{\partial^j X_{00}}{\partial x^{j-k}\partial y^k}=\frac{1}{2\pi}\sum_n\sum_m(-i)^{m+j+1}\frac{(n+j+1)!}{(n-m)!}a^{n+2}z^{-n-j-2}(a_n^m p_{jk}^m+b_n^m q_{jk}^m), \qquad (1)$$

$$\frac{\partial^j Y_{00}}{\partial x^{j-k}\partial y^k}=\frac{1}{2\pi}\sum_n\sum_m(-i)^{m+j+1}\frac{(n+j+1)!}{(n-m)!}a^{n+2}z^{-n-j-2}(a_n^m r_{jk}^m+b_n^m s_{jk}^m), \qquad (2)$$

where $$\left.\begin{matrix}p_{jk}^m\\ q_{jk}^m\end{matrix}\right\}=\int_{-\pi}^{\pi}\cos^{j-k+1}u\sin^k u\left.\begin{matrix}\cos\\ \sin\end{matrix}\right. mudu, \quad \left.\begin{matrix}r_{jk}^m\\ s_{jk}^m\end{matrix}\right\}=\int_{-\pi}^{\pi}\cos^{j-k}u\sin^{k+1}u\left.\begin{matrix}\cos\\ \sin\end{matrix}\right. mudu.$$

p, q, r, and s for $2\leqq m$ and j, $k\leqq 3$ are calculated as given in Table I.

Table I

p \ m	0	1	2	q \ m	0	1	2	r \ m	0	1	2	s \ m	0	1	2
p_{00}^m	0	π	0	q_{00}^m	0	0	0	r_{00}^m	0	0	0	s_{00}^m	0	π	0
p_{10}^m	π	0	$\frac{\pi}{2}$	q_{10}^m	0	0	0	r_{10}^m	0	0	0	s_{10}^m	0	0	$\frac{\pi}{2}$
p_{11}^m	0	0	0	q_{11}^m	0	0	$\frac{\pi}{2}$	r_{11}^m	π	0	$-\frac{\pi}{2}$	s_{11}^m	0	0	0
p_{20}^m	0	$\frac{3}{4}\pi$	0	q_{20}^m	0	0	0	r_{20}^m	0	0	0	s_{20}^m	0	$\frac{\pi}{4}$	0
p_{21}^m	0	0	0	q_{21}^m	0	$\frac{\pi}{4}$	0	r_{21}^m	0	$\frac{\pi}{4}$	0	s_{21}^m	0	0	0
p_{22}^m	0	$\frac{\pi}{4}$	0	q_{22}^m	0	0	0	r_{22}^m	0	0	0	s_{22}^m	0	$\frac{3}{4}\pi$	0
p_{30}^m	$\frac{3}{4}\pi$	0	$\frac{\pi}{2}$	q_{30}^m	0	0	0	r_{30}^m	0	0	0	s_{30}^m	0	0	$\frac{\pi}{4}$
p_{31}^m	0	0	0	q_{31}^m	0	0	$\frac{\pi}{4}$	r_{31}^m	$\frac{\pi}{4}$	0	0	s_{31}^m	0	0	0
p_{32}^m	$\frac{\pi}{4}$	0	0	q_{32}^m	0	0	0	r_{32}^m	0	0	0	s_{32}^m	0	0	$\frac{\pi}{4}$
p_{33}^m	0	0	0	q_{33}^m	0	0	$\frac{\pi}{4}$	r_{33}^m	$\frac{3}{4}\pi$	0	$-\frac{\pi}{2}$	s_{33}^m	0	0	0

Accordingly, we have the next relations for the cases $2 \geqq n$

$$\left.\begin{aligned}
-a_1^1-\sqrt{3}\,a_2^1 &= X_{00} \quad , \\
-3a_1^0-6a_2^0+\sqrt{3}\,a_2^2 &= a\partial X_{00}/\partial x \quad , \\
\sqrt{3}\,b_2^2 &= a\partial X_{00}/\partial y \quad , \\
9a_1^1+15\sqrt{3}\,a_2^1 &= a^2\partial^2 X_{00}/\partial x^2 \quad , \\
3b_1^1+5\sqrt{3}\,b_2^1 &= a^2\partial^2 X_{00}/\partial x\partial y \quad , \\
3a_1^1+5\sqrt{3}\,a_2^1 &= a^2\partial^2 X_{00}/\partial y^2 \quad , \\
45a_1^0+135a_2^0-30\sqrt{3}\,a_2^2 &= a^3\partial^3 X_{00}/\partial x^3 \quad , \\
-15\sqrt{3}\,b_2^2 &= a^3\partial^3 X_{00}/\partial x^2\partial y \quad , \\
15a_1^0+45a_2^0 &= a^3\partial^3 X_{00}/\partial x\partial y^2 \quad , \\
-15\sqrt{3}\,b_2^2 &= a^3\partial^3 X_{00}/\partial y^3 \quad ,
\end{aligned}\right\} \qquad (3)$$

and

$$\left.\begin{aligned}
-b_1^1-\sqrt{3}\,b_2^1 &= Y_{00} \quad , \\
\sqrt{3}\,b_2^2 &= a\partial Y_{00}/\partial x \quad , \\
-3a_1^0-6a_2^0-\sqrt{3}\,a_2^2 &= a\partial Y_{00}/\partial y \quad , \\
3b_1^1+5\sqrt{3}\,b_2^1 &= a^2\partial^2 Y_{00}/\partial x^2 \quad , \\
3a_1^1+5\sqrt{3}\,a_2^1 &= a^2\partial^2 Y_{00}/\partial x\partial y \quad , \\
9b_1^1+15\sqrt{3}\,b_2^1 &= a^2\partial^2 Y_{00}/\partial y^2 \quad , \\
-15\sqrt{3}\,b_2^2 &= a^3\partial^3 Y_{00}/\partial x^3 \quad , \\
15a_1^0+45a_2^0 &= a^3\partial^3 Y_{00}/\partial x^2\partial y \quad , \\
-15\sqrt{3}\,b_2^2 &= a^3\partial^3 Y_{00}/\partial x\partial y^2 \quad , \\
45a_1^0+135a_2^0+30\sqrt{3}\,a_2^2 &= a^3\partial^3 Y_{00}/\partial y^3 \quad ,
\end{aligned}\right\} \qquad (4)$$

where it is assumed that $a=z$ as before.

By solving these simultaneous equations (3) and (4) respectively, we can determine a_1^0, a_1^1, ..., where it must be assumed that X_{00}, $\partial X_{00}/\partial x$, ..., X_{00}, $\partial Y_{00}/\partial x$, ... are already given from Taylor expansions of X and Y. In order to determine the magnetic centre, the parameter a should be adjusted then so as to make the potential due to the second degree terms minimum as studied in the case of Z.

3. Magnetic anomalies in dip. Among the absolute measurements of the elements of magnetic field, the measurement of dip is comparatively easy. Hence it is importance for practical use to analyze magnetic anomalies in dip.

If it is supposed that the anomalies in dip are not large, we may take the relation

$$\tan(\theta_n+\Delta\theta) \fallingdotseq \tan\theta_n+\tan\theta_n\left(\frac{\Delta Z}{Z_n}-\frac{\Delta X}{X_n}\right),$$

where X_n and Z_n denote respectively the northward and downward components of the normal magnetic field, θ_n the normal values of dip, ΔX, ΔZ and $\Delta\theta$ denote their changes.

Then, by putting

$$f(\Delta\theta)=\frac{\tan(\theta_n+\Delta\theta)-\tan\theta_n}{\tan\theta_n}$$

we have the relation

$$f(\Delta\theta)=\frac{\Delta Z}{Z_n}-\frac{\Delta X}{X_n}. \qquad (5)$$

Combining (6) of the first paper with (3) of the present paper, we can easily get the next relation

$$\left.\begin{aligned}
&\frac{1}{Z_n}(2a_1^0+3a_2^0)+\frac{1}{X_n}(a_1^1+\sqrt{3}\,a_2^1) &&= f_{00}\ ,\\
&-\frac{1}{Z_n}(3a_1^1+4\sqrt{3}\,a_2^1)+\frac{1}{X_n}(3a_1^0+6a^{z0}-\sqrt{3}\,a_2^2) &&= a\partial f_{00}/\partial x\ ,\\
&-\frac{1}{Z_n}(3b_1^1+4\sqrt{3}\,b_2^1)-\frac{1}{X_n}\sqrt{3}\,b_2^2 &&= a\partial f_{00}/\partial y\ ,\\
&-\frac{1}{Z_n}(12a_1^0+30a_2^0-5\sqrt{3}\,a_2^2)-\frac{1}{X_n}(9a_1^1+15\sqrt{3}\,a_2^1) &&= a^2\partial^2 f_{00}/\partial x^2\ ,\\
&-\frac{1}{Z_n}5\sqrt{3}\,b_2^2-\frac{1}{X_n}(3b_1^1+5\sqrt{3}\,b_2^1) &&= a^2\partial^2 f_{00}/\partial x\partial y\ ,\\
&-\frac{1}{Z_n}(12a_1^0+30a_2^0+5\sqrt{3}\,a_2^2)-\frac{1}{X_n}(3a_1^1+5\sqrt{3}\,a_2^1) &&= a^2\partial^2 f_{00}/\partial y^2\ ,\\
&-\frac{1}{Z_n}(45a_1^1+90\sqrt{3}\,a_2^1)-\frac{1}{X_n}(45a_1^0+135a_2^0-30\sqrt{3}\,a_2^2) &&= a^3\partial^3 f_{00}/\partial x^3\ ,\\
&-\frac{1}{Z_n}(15b_1^1+30\sqrt{3}\,b_2^1)+\frac{1}{X_n}15\sqrt{3}\,b_2^2 &&= a^3\partial^3 f_{00}/\partial x^2\partial y\ ,\\
&-\frac{1}{Z_n}(15a_1^1+30\sqrt{3}\,a_2^1)-\frac{1}{X_n}(15a_1^0+45a_2^0) &&= a^3\partial^3 f_{00}/\partial x\partial y^2\ ,\\
&-\frac{1}{Z_n}(45b_1^1+90\sqrt{3}\,b_2^2)+\frac{1}{X_n}15\sqrt{3}\,b_2^2 &&= a^3\partial^3 f_{00}/\partial y^3\ .
\end{aligned}\right\} \qquad (6)$$

The coefficients of the spherical hprmonic expansion are determined as the solutions of these simultaneous equations.

4. Actual example. Y. Kato[2] observed repeatedly the changes in magnetic dip in the vicinity of the epicentral area after the Shizuoka Earthquake of July 11, 1935. The differences of the values obtained in the survey in Aug. from that in July are reproduced in Fig. 1. In like manner with the treatment in the case of Volcano Miyakesima in the first report, $\Delta\theta$ was read off from the map from which f_{00}, $\partial f_{00}/\partial x$, ... are calculated by means of least square. From the relation $Z_0=0$, the parameter a was determined to be 4.2 km. The position of the magnetic centre or dipole was marked with a small circle on the map. The north seeking end of the dipole directs toward E7°S. Its dip is also obtained to be 7°. The moment amounts to 4.4×10^{15} emu. The result agreed well with Kato's study in which he determined the position, direction and intensity of the corresponding dipole by means of trial and error method. However, it is not clear why the changes in geomagnetism as obtained here took place in connexion with earthquake occurrence.

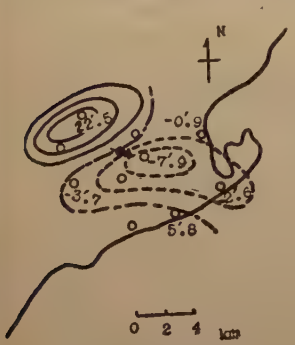

The changes in dip after the Shizuoka Earthquake. (After Y. Kato)

6. Conclusion

The writer showed in this paper that the position, direction and intensity of a subterranean magnetic dipole can be found directly from the anomalies in dip as well as in Z that was already studied in the first report. Applying the method to the anomalies in dip in the case of Shizuoka Earthquake of July, 1935, some interesting results were obtained.

(Read: May 22, 1950)

References

1) T. Rikitake, Journ. Geomag. Geoelectr. **2**, 20 (1950).
2) Y Kato. Sci. Rep. Tohoku Univ. **27**, 1 (1939).

Magnetic Transition Points of Volcanic Rocks*

By Takeshi NAGATA and Syun-iti AKIMOTO

Geophysical Institute, Tokyo University

The knowledge of the magnetic properties of rocks composing the earth's crust is essentially significant in the studies of secular variation and local anomaly of geomagnetic field. Among various magnetic properties of rocks, the magnetic transition points is the most fundamental one. Consequently the change in magnetic susceptibility with temperature of rocks has been examined by a few investigators. (1) (2) (3). In the present study, the thermal change of susceptibility of a large number of volcanic rocks was measured by means of a ballistic method in a weak magnetic field, several times as much as the geomagnetic field. The specimens examined were thirty in total and they are the ejecta from volcanoes Huzi, Amagi, Mihara, Usame, Hakone, and Taga, each of which was analysed chemically and petrologically by petrologists. These specimens were heated up to about 660°C and then cooled down to the room-temperature. During the heating and cooling processes, their susceptibility was measured every 20°C.

The results of this experiments show that the susceptibility of all specimens becomes apparently zero at about 600°C, which coincides with the Curie-point of pure magnetite. The mode of change with temperature, however, is not simple. Its thermal change seems to be classified, generally speaking, into the four types such as given in Figs. 1—4, as the typical examples. In Fig. 1, the susceptibility in heating process increases grandually up to about 400°C and then decreases abruptly, and the change

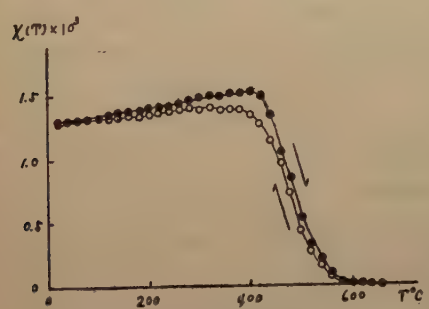

No. 1. H=2.13 O_e.
(No. 23) Huji

Fig. 1. Reversible ordinary type

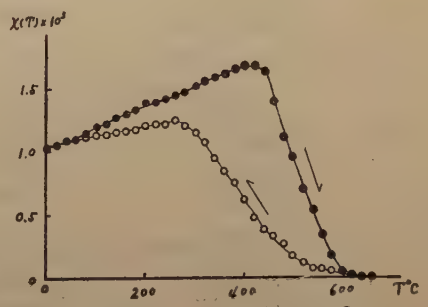

No. 2. H=1.80 O_e.
(No. 55) Usami

Fig. 2. Irreversible ordinary type

---

* Contribution from Division of Geomagnetism and Geoelectricity, Geophysical Institute, Tokyo University, Series II, No. 9.

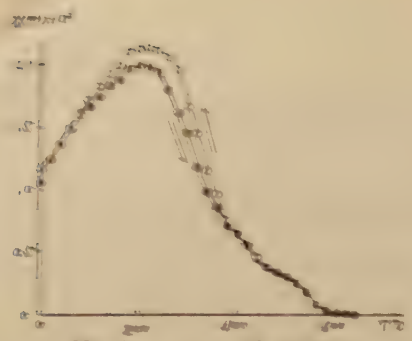

No. 3. $H=1.80\ O_e$.
(No. 38) Mihara

Fig. 3. Reversible extraordinary type

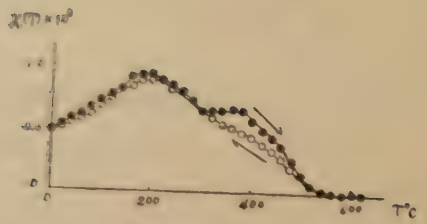

No. 4. $H=1.80\ O_e$.
(No. 82) Haeone

Fig. 4. Irreversible extraordinary type

in cooling process follows almost the same curve: this change will be called "reversible ordinary type". In Fig. 2, the change in heating process is similar to that in Fig. 1,

REVERSIBLE TYPE

Table 1

Specimen No.	Locality	Rock	χ_0	χ_{max}
17	Ōsumi Hoei crater	Olivine-basalt	2.25×10^{-3}	2.56×10^{-3}
18	Ōsumi Makurawa 1	Hypersthene-augite-olivine-basalt	1.31	2.06
19	Ōsumi Tawaramonaki	Olivine-basalt	1.82	2.75
20	Ōsumi Makurawa 2	Olivine-basalt	1.28	1.42
22	Ōsumi Makurawa 3	Augite-bearing olivine-basalt	1.55	1·93
22	Ōsumi Hoei bomb	Augite-bearing olivine-basalt	0.70	1.08
23	Ōsumi Makurawa 4	Two-pyroxene-bearing olivine-basalt	1.29	1.46
24	Ōsumi Kurusuiwa	Aphanitic andesite	0.40	0.68
25	Ōsumi Aokigahara	Two-pyroxene-olivine-basalt	0.90	2.05
29	Amagi Enokubo-yama	Olivine-basalt	0.78	1.42
30	Amagi Inamuro	Olivine-bearing two-pyroxene-andesite	1.06	1.60
32	Amagi Yamagase	Two-pyroxene-andesite	0.63	0.79
33	Amagi Yakano-yama	Olivine-bearing two-pyroxene hornblend-dacite	0.89	1.15
34	Amagi Akazawa	Olivine-two-pyroxene bearing andesite	0.54	0.96
35	Ōsumi Ōsuna	Hypersthene-bearing olivine-basalt	0.38	0.42
36	Ōsumi Somma of Mihara	Hypersthene-bearing olivine-basalt	1.86	2.48
37	Ōsumi Ame lava	Hypersthene-bearing basalt	1.76	3.34

while its cooling does not accord with the heating one, the change will be named "irreversible ordinary type". On the other hand, in Fig. 3 and Fig. 4, the thermal change of susceptibility is stepwise, the former reversible and the latter irreversible; these types will be called respectively "reversible and irreversible extraordinary type".

As the magnetic transition points, two points on the temperature scale were taken: the one is the temperature denoted by Θ_a at which ferromagnetism of rocks disappears, while the other is the temperature denoted by Θ_m at which $-\frac{\delta}{\delta T}\chi(T)$ maximum. (4). These characteristic quantities of the measured 35 specimens were given in Table 1, and Table 2, where χ_0, χ_{max}, and $T_{\chi=max}$ denote respectively initial specific susceptibility at 0°C, maximum specific susceptibility, and the temperature corresponding to the maximum specific susceptibility. Suffixes o and e represent the ordinary and the extraordinary types. Reversible types were summarized in Table 1, while irreversible ones in Table 2.

$T_{\chi=max}$	Θ_{ao}	Θ_{ae}	Θ_{mo}	Θ_{me}	Fe_2O_3	FeO	TiO_2
300°C	580°C		460°C		5.40%	6.65%	1.46%
210	580	320	520	285	2.76	7.72	1.41
170	580	300	530	235	3.67	9.86	1.97
380	580		500		4.50	6.89	1.73
410	590		515		4.78	5.72	1.38
190	580	310	520	260	2.64	8.42	1.38
390	580		495		3.04	7.29	1.15
200	585	300	530	230	0.96	5.02	0.27
140	585	290	530	195	1.23	8.34	1.43
160	590	280	530	200	1.92	6.77	1.03
200	610		530		3.03	3.30	0.36
300	595		520		2.66	3.40	0.85
350	600		490		1.25	2.52	0.40
220	580	400	550	290	1.54	7.00	0.79
440	580		550		2.13	7.05	0.71
320	600		450		4.13	8.30	0.43
180	595	390	530	270	4.60	10.08	1.39

◦38	Oosima Meizi-Taisyo lava	Basalt	1.06	2.06
51	Usami	Two-pyroxene-andesite	0.45	0.84
56	Usami	Augite-hypersthene-andesite	0.64	0.87
91	Taga	Augite-olivine-basalt	1.10	2.02

Table 2

IRREVERSIBLE TYPE

Specimen No.	Locality	Rock	χ_0	Heating χ_{max}	Heating $T_{\chi=max}$
27	Amagi Zizodo	Olivine-basalt	1.28×10^{-3}	2.41×10^{-3}	360°C
49	Usami	Olivine-two-pyroxene-andesite	0.99	1.44	360
50	Usami	Aphyric-two-pyroxene-andesite	0.94	2.06	440
52	Usami	Hypersthene-bearing olivine-augite-andesite	1.04	1.27	440
53	Usami	Augite-bearing olivine-hypersthene andesite	0.54	0.67	320
54	Usami	Olivine-bearing two-pyroxene andesite	0.84	1.43	400
◦55	Usami	Olivine-bearing two-pyroxene andesite	1.02	1.69	420
◦82	Hakone New somma	Hypersthene-augite-andesite	0.48	0.94	180
93	Taga	Two-pyroxene olivine-basalt	0.70	1.04	280

It seems clear that the magnetic transition points depend upon the chemical constitution of the rock. In order to see the relation mentioned above, Θ_m of variors specimens were plotted against the ratio Fe_2O_3/Fe_2O_3+FeO in Fig. 5. As for Θ_m of the specimen, Being stepwise in the thermal change of its susceptibility, the lower curie-point, Θ_{mc}, was adopted. The adove ratio is to be 0.69 for the pure magnetite. In the valcanic rocks, however, FeO is involved in not only magnetite but in hypersthene and olivine usually, and so this ratio is inferior to 0.69. As will be seen in Fig. 5, Θ_m decreases as the relative amount of FeO increases. In general, some amounts of TiO_2 may be contained in the ordinary natural magnetite and Fe_2O_3, FeO, TiO_2 may compose various kinds of solid solution, so that TiO will play a remarkable role in ferromagnetic mineral: that is relative amount of Fe_2O_3 but on TiO_2 probably.

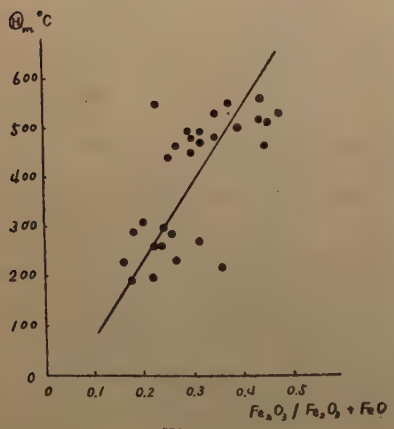

Fig. 5

210	590	420	550	310	2.69	10.57	0.74
210	620	370	570	220	2.61	4.61	0.82
430	600		550		3.48	5.70	0.73
260	600	420	520	300	2.54	7.92	0.87

Cooling χ_{max}	Coolnig $T_{\chi=max}$	Θ_{ao}	Θ_{ae}	Θ_{mo}	Θ_{me}	Fe_2O_3	FeO	Ti_2O
2.22×10^{-3}	260C°	H600°C C620		H460C° C320		2.89%	7.66%	0.64%
1.27	280	H620 C620	530°C	H470 C530	360°C	2.76	6.03	0.73
1.47	280	H630 C630		H560 C550		4.60	5.90	1.04
1.27	280	H580 C600		H470 C410		3.18	6.73	0.85
0.62	340	H600 C600	560	H530 C570	420	2.79	5.28	0.71
1.10	280	H620 C620		H490 C360		3.25	6.97	0.92
1.26	260	H620 C620		H480 C390		3.18	7.25	0.76
0.89	200	H550 C560	420	H470 C300	260	1.13	3.86	0.72
0.87	220	H640 C640		H440 C300		2.45	7.13	0.67

In the present study, we see that the ordinary type change is caused from magnetite grains containing some amounts of impurities, while as for the extraordinary type we could not clearify its original ferromagnetic mineral.

References

(1) R. Chevallier et J. Piere. Ann de phys. **18**, 383 (1932).
(2) T. Nagata, Bull. Earthq. Res. Inst., **19**, 579 (1941).
(3) H. Manley, Thesis, (Univ. of London,) June (1949).
(4) T. Nagata, Bull, Earthq. Res. Inst., **21**, 45 (1943).

LETTER TO EDITOR

An Estimation of Diurnal Variation of VHF Radio Waves.

In this letter, the writer reports that the diurnal variation in the vertical distribution of the refractive index due to the variation in meteorogical conditions, is expected to be the main cause of the diurnal variation of VHF radio waves.

In the lit-zone, the receiving electric field are mainly composed of the direct wave, the reflected wave from the ground and the ground wave, and are shown by the Bullington's formula,

$$\frac{E}{E_0}=2\sin\frac{A}{2}+j\left[(1+R)+(1-R)A\right]e^{j\left(\frac{A}{2}\right)},$$

where E_0 is the free-space field intensity.

The variation in the vertical distribution of refractive index changes the wave path and reflection angle. For this reason, the receiving electric field changes.

In actual cases, the vertical gradients of $(n-1)\times10^6$/km are often 50 in night and 40 in daytime respectiAely, in the lower atmosphere, where n is the refractive index. In this case, the ranges of diurnal variation are theoretically given as follows.

Range	Polarization	Medium under path
5 db	Vertical	Land
3	Horizontal	Land
8	Vertical	Sea
4	Horizontal	Sea

wave-length; 5 m
distance; 110 km
antenna height; 200 m

These range agrees with the experimental results in its order of magnitude. In near future, the experimental proof will be given.

By Kunio Hirao
Central Radio Wave Observatory.
(June 27, 1950)

The Meeting of the Society of Terrestrial Magnetism and Electricity.

The 7th General Meeting. Held at the Tokyo University on May 22–24, 1950. 70 Reports were read, 150 Members assembled.

The Tanakadate-prize were awarded for the following excellent workers.

The 6th, Mr. S. Matsushita and Mr. Y. Aono:
On the Movement of the Electrical State in the Ionosphere.
The 7th, Mr. M. Sugiura and Mr. G. Ishikawa:
On the Screening Effect by the Ionosphere.

昭和25年9月25日 印刷
昭和25年9月31日 發行
第2卷第1號　定價150圓

編輯兼發行者　日本地球電氣磁氣學會
代表者　長谷川万吉

印刷者　京都市下京區上鳥羽學校前
田中幾治郎

賣捌所　丸善株式會社京都支店
丸善株式會社　東京・大阪・名古屋・仙台・福岡

JOURNAL OF GEOMAGNETISM AND GEOELECTRICITY

Vol. II No. 1

1950

CONTENTS

On the Influence of the Hall Current to the Electrical Conductivity of the Ionosphere. I, ... M. HIRONO 1

Circulatory Motions in the Ionospheric Atmosphere and their Relation to the S Field of the Terrestrial Magnetism. III, ...S. MATSUSHITA 9

Magnetic Anomalies and the Corresponding Magnetic Centres. I, ...
T. RIKITAKE 20

Magnetic Anomalies and the Corresponding Magnetic Centres. II, ...
T. RIKITAKE 25

Magnetic Transition Points of Volcanic Rocks, ...
T. NAGATA and S. AKIMOTO 29

LETTER TO EDITOR:

An Estimation of Diurnal Variation of VHF Radio Waves,....K. HIRAO 34